EXHIBIT A

Journal of Neurochemistry, 2001, 79, 426–436

Survivin inhibition induces human neural tumor cell death through caspase-independent and -dependent pathways

Sai Latha Shankar,* Sridhar Mani,† Kathleen Norman O'Guin,* Ekambar R. Kandimalla,‡ Sudhir Agrawal‡ and Bridget Shafit-Zagardo*

*Departments of *Pathology and †Oncology, Albert Einstein College of Medicine, Bronx, New York, USA*
‡Hybridon Inc., Cambridge, Massachusetts, USA

Abstract

Survivin inhibits apoptosis during development and carcinogenesis and is absent in differentiated cells. To determine whether survivin inhibition induces cell death in neural tumor cells, survivin antisense oligonucleotides (SAO) were administered to a human neuroblastoma (MSN) and an oligodendroglioma (TC620) resulting in a dose-dependent reduction in survivin protein. Although 74% of the SAO-treated MSN cells were trypan blue$^+$, PARP cleavage or activated caspase-3 was not observed. However nuclear translocation of AIF occurred and XIAP increased dramatically. Co-administration of z-Val-Ala-Asp(OMe)-fluoromethyl ketone (zVAD-fmk) with SAO did not inhibit cell death suggesting a caspase-independent mechanism of cell death. Propidium iodide (PI) staining revealed multiple large macronuclei with no apoptotic bodies supporting a role for survivin in cell division. By contrast, while 70% of the SAO-treated TC620 cells were trypan blue$^+$, PARP was cleaved, cells were TUNEL$^+$ and PI-staining revealed macronuclei and numerous apoptotic bodies. Co-treatment of the TC620 cells with SAO and zVAD-fmk blocked cell death. While no macronuclei or apoptotic bodies were observed there was a two-fold increase in metaphase cells. Our results suggest that survivin inhibition decreases the viability of human neural tumor cells and as a result of mitotic catastrophe, cell death can be initiated by either a classic apoptotic mechanism or a caspase-independent mechanism.

Keywords: antisense oligonucleotides, apoptosis, cell death, human brain tumors, survivin.

J. Neurochem. (2001) **79**, 426–436.

Members of anti-apoptotic gene families such as the bcl-2 family and the inhibitor of apoptosis (IAP) family are often up-regulated in brain tumors where their role in blocking apoptosis contributes to tumor progression (LaCasse *et al.* 1998; Leaver *et al.* 1998; Deininger *et al.* 1999). Human survivin, one of seven IAP family members, is increased in abundance in neuroblastomas and portends poor prognosis (Adida *et al.* 1998). Neuroblastomas often have a gain in the distal region of 17q suggesting that survivin expression at 17q25 may contribute to tumor pathogenesis (Islam *et al.* 2000).

Survivin is cell cycle regulated and increased during the G2/M phase of the cell cycle. During G2/M survivin associates with and is phosphorylated by cdc2/cyclin B1 and subsequently binds to tubulin on the mitotic spindle (Li *et al.* 1998; O'Connor *et al.* 2000). Survivin also associates with the midbody, kinetochore (Li *et al.* 1998; Skoufias *et al.* 2000), and binds cdk4 to aid in the G1/S transition (Suzuki *et al.* 2000) implicating survivin with normal G2/M and G1/S checkpoint transitions and mitosis.

The purpose of this study was to determine whether survivin was expressed in a variety of neural tumors and whether survivin antisense oligonucleotides (SAO) could down-regulate survivin in neural cell lines and induce tumor cell death. In lung and colon carcinomas (Chen *et al.* 2000;

Received June 26, 2001; revised manuscript received August 3, 2001; accepted August 6, 2001.

Address correspondence and reprint requests to Dr Bridget Shafit-Zagardo, Department of Pathology, Forchheimer 524, Albert Einstein College of Medicine, 1300 Morris Park Avenue, Bronx, NY 10461, USA. E-mail: zagardo@aecom.yu.edu

Abbreviations used: AIF, apoptosis-inducing factor; DAPI, 4′,6-diamidino-2-phenylindole; DTT, dithiothreitol; FCS, fetal calf serum; DMSO, dimethyl sulfoxide; IAP, inhibitor of apoptosis; PARP, poly-(ADP-ribose)-polymerase; PI, propidium iodide; SAO, survivin antisense oligonucleotides; SDS–PAGE, sodium dodecyl sulfate–polyacrylamide gel electrophoresis; TBS, Tris-buffered saline; TRITC, tetramethylrhodamine isothiocyanate; TUNEL, TdT-mediated dUTP nick-end labeling; XIAP, X-linked inhibitor of apoptosis; zVAD-fmk, z-Val-Ala-Asp(OMe)-fluoromethyl ketone.

© 2001 International Society for Neurochemistry,

Olie *et al.* 2000) survivin down-regulation induced apoptosis, however, survivin levels are higher in neuroblastomas (Islam *et al.* 2000). We have determined that SAO down-regulated survivin protein resulting in caspase-independent cell death in a neuroblastoma cell line, while an oligodendroglioma cell line underwent caspase-dependent apoptotic cell death.

Materials and methods

Cell culture conditions

Cells were grown in a humidified atmosphere containing 5% (HOG, TC620) or 8% (MSN, HTB 14, HTB 17) CO_2 at 37°C. MSN cells were grown in RPMI 1640 supplemented with 23.8 mM sodium bicarbonate, 10% fetal calf serum (FCS), 0.1 mM non-essential amino acids, 0.47 mM L-serine and 0.38 mM L-asparagine (Reynolds *et al.* 1986). TC620 and HOG were maintained in Iscove's medium plus 10% FCS (Dr Anthony Campagnoni; UCLA). HTB 14 and the HTB 17 were maintained in DMEM plus 10% FCS (ATCC). Jurkat cells served as a positive control for survivin immunoblotting (Conway *et al.* 2000) and were grown in RPMI 1640 plus 10% FCS.

RNA isolation and northern blot analysis

Total RNA was isolated from the cell lines using TRI-reagent (Molecular Research Center; Cincinnati, OH, USA). Northern blot analysis and primings were performed as previously described (Shafit-Zagardo *et al.* 1988). The probes were labeled using [α-^{32}P]-dCTP and the Multiprime DNA labeling system (Amersham, Arlington Heights, IL, USA).

Oligonucleotide treatments

Eleven different antisense phosphorothioate oligonucleotides to the survivin gene (Genbank accession number U75285) and two mismatched phosphorothioate oligonucleotides were designed based on the selection criteria described earlier (Agrawal and Kandimalla 2000). The antisense oligonucleotides were synthesized on solid support with an automated DNA synthesizer using β-cyanoethyl-phosphoramidite chemistry. To prevent rapid degradation of the oligonucleotides by cellular nucleases, oxidation was performed with Becauge sulfurizing agent to obtain phosphorothioate backbone modified oligonucleotides. After their synthesis, the oligonucleotides were released from the solid support, deprotected, purified by reverse-phase HPLC, desalted, filtered and lyophilized. The purity and sequence integrity of oligonucleotides was ascertained by capillary gel electrophoresis and MALDI-TOF mass spectral analysis and the concentrations measured at 260 nm. The sequences of eight oligonucleotides used in this study are shown in Table 1. Cells were grown in 100-mm dishes and oligonucleotide treatment was performed for 48 h on subconfluent cultures in the presence of lipofectin (Gibco, Rockville, MD, USA).

Protein preparation and immunoblotting

Total protein homogenates were prepared as previously described (Albala *et al.* 1995). Equal amounts of protein (100 μg; Biorad detection system, Bio-Rad Laboratories, Hercules, CA, USA) were analyzed by SDS–PAGE on 10% gels (Laemmli 1970) and electrophoretically transferred to nitrocellulose (Towbin *et al.* 1979). To demonstrate specificity during immunoblotting, human survivin GST-fusion protein (10 μg) was used to absorb the survivin polyclonal antibody overnight (1 : 500) at 4°C prior to immunoblotting. Immunoblots were blocked with 5% non-fat, dry milk in 1 × Tris-buffered saline (TBS) (0.14 M NaCl, 0.001 M Tris, pH 7.4). Blots were cut at 32.9 kDa and the bottom were incubated with the survivin antibody overnight at 4°C and visualized by enhanced chemiluminescence (ECL; Amersham). The top part of the blots was incubated with a β-tubulin antibody (TUB 2.1; Sigma, St Louis, MO, USA) overnight at 4°C. Two survivin polyclonal antibodies yielded identical results (R & D Systems, Inc., Minneapolis, MN, USA; Alpha Diagnostics International, San Antonio, TX, USA). The XIAP mAb was purchased from StressGen Biotechnologies Corp. (Victoria, BC, Canada). The poly-(ADP-ribose)-polymerase (PARP) mAb was from Pharmingen (San Diego, CA, USA).

Trypan blue exclusion assay

Cells were harvested 48 h after SAO treatment, stained with 0.04% Trypan blue (Gibco) and both non-viable (trypan blue positive) and viable (trypan blue negative) cells were counted on a hemocytometer. A minimum of 250 cells were counted for each data point. The data was expressed as a percentage of dead cells relative to the total cell number. Individual experiments were performed in triplicate. MSN studies were performed three times, while TC620 studies were performed twice.

Caspase-3 activity assay

MSN cell pellets were washed twice in cold PBS and resuspended

Table 1 Sequences of 20-mer phosphorothioate survivin antisense oligonucleotides

HYB oligonucleotide number	Sequence (5′→ 3′)	Target site
900	d(GCCAGTTCTTGAATGTAGAG)	2867–2886
901	d(CAGTGGATGAAGCCAGCCTC)	3180–3199
903	d(CCCTAGCTCACACTCTCATT)	4385–4404
904	d(TCTTGGCTCTTTCTCTGTCC)	5248–5267
905	d(GAGCCTTCCTCTTCATGTCC)	11432–11451
906	d(GCTTCCCAGTCACATCCTGT)	11897–11916
908	d(GCCACTGTTACCAGCAGCAC)	12241–12260
1132	d(GCACCTAGTCTCCCTGCACC)	Mismatched oligo

in ice-cold hypotonic cell lysis buffer (25 mM HEPES, pH 7.5, 5 mM $MgCl_2$, 5 mM EDTA, 5 mM DTT, 2 mM PMSF, 10 μg/mL pepstatin A, 10 μg/mL leupeptin), incubated on ice for 20 min, sonicated briefly and centrifuged at 11 000 *g* for 20 min at 4°C. Supernatant (50–100 μg) was incubated in caspase-3 assay buffer [100 mM HEPES, pH 7.5, 10% sucrose, 0.1% CHAPS and 10 mM dithiothreitol (DTT)], 2 μL of dimethyl sulfoxide (DMSO), 100 mM DTT in a final volume of 100 μL at 30°C for 30 min in black opaque 96-well plates (USA Scientific Inc; Orlando, FL, USA). Subsequently, 2 μL of the caspase-3 substrate Ac-DEVD-AMC (50 μM, Pharmingen) was added to each well. Plates were incubated at 30°C for 60 min in the dark. Fluorescence of the reaction was measured at an excitation of 355 nm and an emission of 460 nm with a cut-off filter of 455 nm using a SPECTRAmax GEMINI spectrofluorometer with SOFTmax® PRO software (Molecular Devices; Sunnyvale, CA, USA). Assays were performed in triplicates. The data is presented as mean relative fluorescence units/mg protein ± SD. The negative controls included the caspase-3 inhibitor Ac-DEVD-CHO that eliminated caspase-3 activation.

Propidium iodide (PI) staining

SAO-treated cells were fixed with 4% paraformaldehyde for 30 min at room temperature, washed with 1 × TBS, permeabilized with 0.1% Triton X-100 for 30 min and treated with 10 μg/mL DNase free RNase A (Sigma) for 60 min. Nuclei were stained with 200 μg/mL PI for 30 min at 4°C and washed twice with 1 × TBS. Nuclear morphology was assessed on an inverted Olympus IX70 fluorescence microscope equipped with phase and epifluorescence optics. For each treatment about 600 nuclei were scored as normal, condensed, or abnormal on 15 random, 40 × objective fields in duplicate.

TUNEL assay

The TUNEL assay was performed to assess apoptotic cell death in SAO-treated TC620 cells using the In Situ Cell Death Detection Kit, Fluorescein (Roche Molecular Biochemicals, Indianapolis, IN, USA). The TUNEL reaction preferentially labels cleaved genomic DNA generated during apoptosis, by the addition of fluorescein dUTP at strand breaks. Lipofectin, mismatch 1132 or SAO-treated TC620 cells were fixed and permeabilized as described for PI staining. Cells were washed and incubated in the TUNEL reaction mixture, prepared according to the manufacturer's recommendations, for 1 h at 37°C. Omission of the terminal deoxynucleotidyl transferase in the label solution served as a negative control for the TUNEL fluorescence staining. Cells were washed twice and counterstained with the DNA specific dye DAPI (1 : 1000 of a 1 mg/mL stock; 15 min at room temperature). Cells were examined with an Olympus IX70 inverted microscope. For each treatment 15 random, 40 × objective fields consisting of ~1000 cells were examined in duplicate chamber slides. TUNEL-positive nuclei were expressed as a percent of the total number of cells per individual field.

Apoptosis-inducing factor (AIF) immunostaining and quantitation

Lipofectin, mismatch 1132 or SAO-treated MSN cells were fixed and permeabilized as described for PI staining, and blocked for 1 h at room temperature with 10% normal goat serum in 5% non-fat, dry milk in 1 × TBS. The cells were incubated with an AIF polyclonal antibody (1 : 100; Santa Cruz Biotechnology Inc, Santa Cruz, CA, USA) overnight at 4°C, and revealed with a goat anti-rabbit IgG conjugated to TRITC (Southern Biotechnology Associates, Birmingham, AL, USA). Omission of the primary antibody confirmed that the immunostaining was specific. Cells were counterstained with the DNA-specific dye DAPI (1 : 1000 of a 1 mg/mL stock; 15 min at room temperature). Cells were examined with an Olympus IX70 inverted microscope. Fluorescent images were collected using a 12-bit Photometrics cooled CCD camera. For each treatment, 15 random, 40 × objective fields consisting of ~600 cells were examined. TRITC (red) and DAPI (blue) stained cells were scored as having AIF staining either in the mitochondria or the nucleus relative to the total cell number examined. In parallel, the DAPI stained nuclei were also scored as normal, condensed, or abnormal nuclei. Experiments were performed in duplicate.

Results

Expression of survivin in human neural tumor cell lines

Northern and western blot analysis were performed to verify survivin expression in human neural tumor cell lines derived from a human neuroblastoma (MSN), two oligodendrogliomas (HOG and TC620), an astrocytoma (HTB17) and a glioblastoma (HTB14). Northern blot analysis revealed the expression of the 1.9 kb survivin transcript in the five neural tumor lines examined (Fig. 1a). When normalized to 18S RNA, higher expression of survivin was found in the two oligodendroglioma cell lines, while the neuroblastoma, glioblastoma and the astrocytoma showed comparable survivin expression. Immunoblotting confirmed the presence of the 16.5-kDa survivin protein in all neural tumor lines (Fig. 1B). When normalized to β-tubulin, survivin protein levels were three-fold higher in the HTB-14, MSN and the HTB-17 homogenates relative to the HOG cell homogenate. Examination of two additional neuroblastomas (IMR32 and SK-N-SH; data not shown) and the oligodendroglioma (TC620; Fig. 2b) also confirmed the presence of survivin. To verify the specificity of the survivin antibody, identical protein blots were incubated with the survivin antibody preincubated with the GST–survivin fusion protein. Absorption of the antibody eliminated survivin immunoreactivity (Fig. 1B).

Regulation of survivin expression at G2/M cell cycle checkpoints

As shown in Fig. 2(a), a 1.7–2.6-fold increase in survivin protein was observed in total cell lysates from MSN cells treated with three G2/M checkpoint blockers relative to the DMSO control. A similar 1.6-fold increase in survivin protein was observed in the nocodazole-treated TC620 cells (Fig. 2b) demonstrating that in neural tumor cell lines survivin expression is increased in a G2/M cell cycle phase-dependent manner. In contrast, cells treated with agents such as flavopiridol that typically block cells in G1/S (Carlson

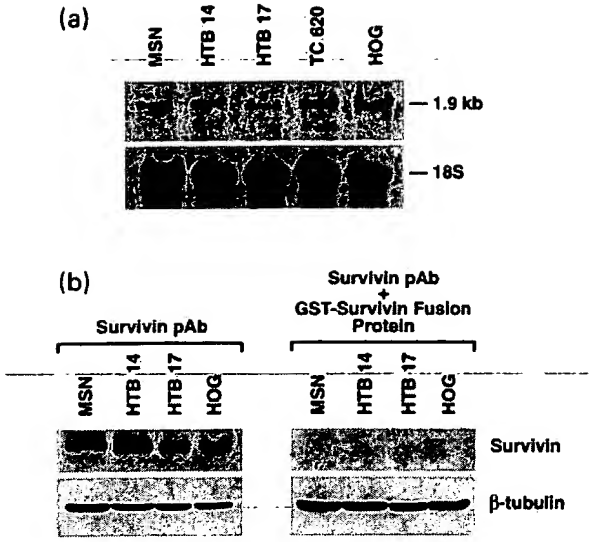

Fig. 1 Survivin is expressed in human brain tumors. (a) Total RNA (30 μg) were run on a 1% agarose–formaldehyde gel and transferred to nitrocellulose. The blot was first hybridized with a cDNA probe to the entire coding region of the survivin gene and subsequently hybridized with a cDNA to 18S. The survivin RNA expression was normalized to the expression of 18S RNA. The relative amounts were MSN, 0.075; HTB-14, 0.11; HTB-17, 0.065; TC620, 0.25; HOG, 0.25. (b) Total protein was isolated from MSN, HTB 14, HTB 17 and HOG cells. The blots were cut at 32.9 kDa and was incubated with a β-tubulin mAb (1 : 1000) to confirm equal loading. The lower halves were incubated with a survivin polyclonal antibody (1 : 500) or with the survivin polyclonal antibody (1 : 500) pretreated with 10 μg of GST-survivin fusion protein. Blots were scanned in the linear range and data was presented as a ratio of survivin over tubulin in each cell type. The relative quantities were MSN, 0.35; HTB-14, 0.45; HTB-17, 0.39; HOG, 0.13. Two independent experiments were performed and consistent results were obtained.

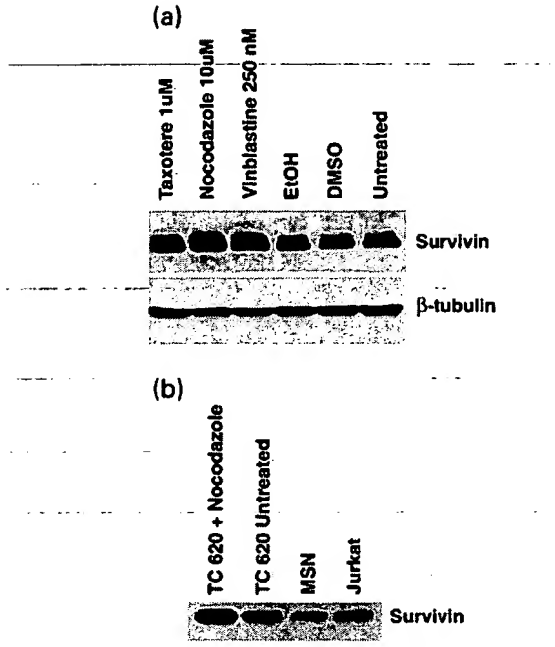

Fig. 2 Survivin protein increases following treatment with G_2/M checkpoint blockers. (a) G_2/M cell cycle checkpoint blockers elevate survivin protein expression. Total protein was isolated from MSN cells either untreated or treated with vinblastine (250 nM), nocodazole (10 μM) or taxotere (1 μM) for 16 h. DMSO and ethanol (EtOH) were added as carriers. In each of the treatments, the increase of survivin protein relative to DMSO or EtOH was vinblastine, 1.9-fold; nocodazole, 2.6-fold; taxotere, 1.7-fold. (b) Total protein was isolated from nocodazole-treated (10 μM, 24 h) and untreated TC620 cells, MSN cells and Jurkat cells. A 1.6-fold increase in survivin protein was observed on the nocodazole-treated TC620 cells. Three independent experiments were performed and consistent results were obtained.

et al. 1996; our data) did not alter survivin protein abundance (data not shown).

In MSN cells, SAO decrease survivin protein abundance, do not activate caspase-3 and undergo caspase-independent cell death

To determine whether the inhibition of survivin was sufficient to induce cell death in nervous system tumors, 11 SAO spanning the survivin gene were analyzed in MSN and TC620 cell lines. Seven SAO and the mismatch oligonucleotide used in this study are shown in Table 1. As shown in Fig. 3(a), SAO 904 treatment decreased survivin protein levels in MSN cells in a dose-dependent manner. At 400 and 600 nM, SAO 904 decreased survivin protein levels by 46% and 60% while survivin levels were unchanged in cells incubated with the mismatched oligonucleotide 1132. By contrast, treatment with SAO 908 that binds within the 3′-untranslated region of the survivin mRNA did not result in a significant decrease in survivin protein. Examination of other SAO in the MSN cells showed that 901, 903, 904 and 906 (400 nM) were most effective in decreasing survivin protein levels (Fig. 3b). Further, mismatched oligonucleotides had no effect on the relative abundance of survivin.

Survivin's role as an IAP and a survival protein for neuroblastomas was investigated by examining whether the down-regulation of survivin was sufficient to induce cell death in MSN cells. Following transfection with lipofectin, mismatched oligonucleotide 1132 (600 nM) or SAO 904 and 906 (600 nM), the numbers of trypan blue positive cells, indicative of dead cells, were counted 48 h post-treatment. In the presence of 600 nM SAO 904 and 906, the percentage of cells that were trypan blue positive were 73% and 81% (Fig. 3c). Upon treatment with lipofectin or the mismatched oligonucleotide 1132, only 7–11% of the cells were trypan blue-positive. These data therefore demonstrate that the inhibition of survivin following SAO treatment is sufficient to induce cell death in MSN cells.

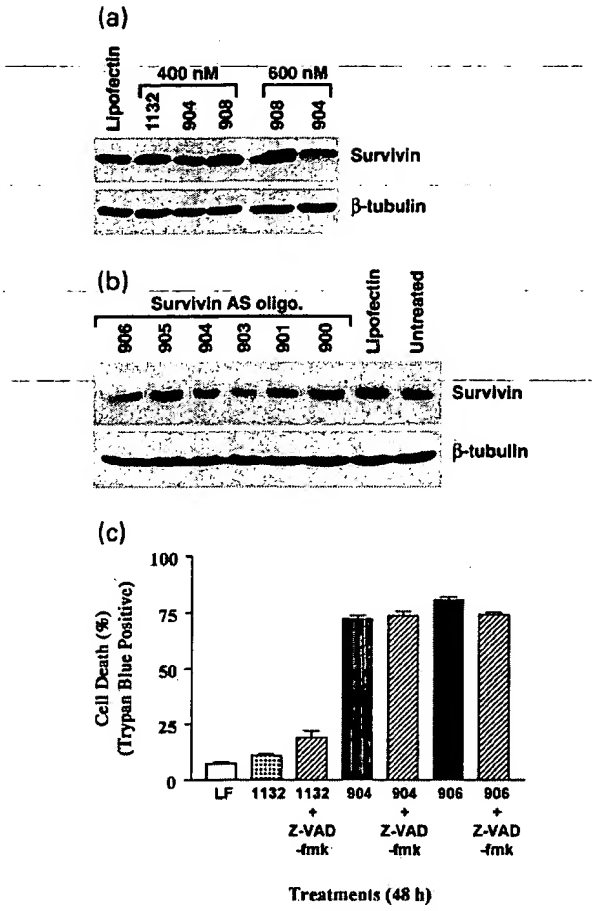

Fig. 3 SAO treatment of MSN cells results in reduced survivin protein levels and increased cell death. (a) MSN cells were treated with lipofectin, SAO 904 and 908 at 400 and 600 nM or mismatched oligonucleotide 1132 at 400 nM. With SAO treatment, the percentage of survivin protein over β-tubulin relative to lipofectin was 904 (400 nM), 54%; 904 (600 nM), 40%; 908 (400 nM), 129%; 908 (600 nM), 91%; 1132 (400 nM), 109%. (b) Six SAOs (900–906) were administered at 400 nM. The percentage of survivin protein over β-tubulin relative to lipofectin was: 900, 77.7%; 901, 38.3%; 903, 24.3%; 904, 35.7%; 905, 55.6%; 906, 26.9%. Three independent experiments were performed. (c) MSN cells treated with lipofectin, 600 nM SAO 904, 906, mismatch oligonucleotide 1132, or co-treated with SAO or 1132 and 20 μM zVAD-fmk for 48 h, were stained with 0.04% trypan blue. The data are expressed as the percentage of dead cells relative to the total cell number ± SEM. Three independent experiments were performed in duplicate.

To determine whether MSN cell death by SAO was mediated by caspase-3 activation, we examined whether PARP was cleaved. Immunoblotting of MSN protein homogenates with a PARP antibody failed to detect PARP cleavage and a single 116-kDa PARP protein band that was not cleaved was observed in MSN cells following SAO treatment for either 24 h or 48 h (data not shown). Also, higher concentrations of SAO failed to cleave PARP. As a result of the PARP data, we examined whether SAO-treated cells have active caspase-3. Previous studies from our laboratory demonstrated that MSN cells activate caspase-3 following staurosporine treatment, and when caspase-3 is activated PARP is cleaved. As shown in Table 2, over a seven-fold increase in caspase-3 activity was observed upon staurosporine treatment of MSN cells, however, no significant increase in caspase-3 activity was observed following SAO treatment. This data was consistent with our PARP immunoblotting data.

We then examined if SAO-induced cell death could be blocked by the broad-spectrum caspase inhibitor z-Val-Ala-Asp(OMe)-fluoromethyl ketone (zVAD-fmk). As shown in Fig. 3(c), SAO 904 and 906 treatment resulted in 73% and 80% trypan blue positive cells and upon incubation of SAO 904 and 906 with zVAD-fmk, 73% and 74% of the cells remained trypan blue positive indicating that inhibiting caspases did not affect cell death. Taken together, the caspase-3, PARP and the zVAD-fmk experimental data suggest that in MSN cells SAO treatment induced cell death in a caspase-independent manner.

Induction of nuclear abnormalities in SAO-treated MSN cells

PI staining and phase microscopy were used to assess the nuclear morphology of the SAO-treated MSN cells. Lipofectin-treated or mismatch oligonucleotide 1132 treated cells showed normal nuclear morphology (Figs 4a and b) consistent with our previous observation that at any given time approximately 5% of MSN cells exhibited abnormal nuclei. By contrast, PI staining of SAO-treated cells revealed a dramatic increase in abnormal appearing nuclei that included multiple, multilobulated nuclei (Figs 4c and e,

Table 2 Caspase 3 is inactive in survivin antisense oligonucleotide-treated MSN cells

Treatment	Time	Relative units/ mg protein ± SD
Lipofectin	48 h	30 556 ± 899
903 (400 nM)	48 h	27 850 ± 2311
904 (400 nM)	48 h	33 532 ± 3732
1132 (400 nM)	48 h	30 961 ± 1681
Staurosporine (1 μM)	6 h	264 281 ± 8130
DMSO control for staurosporine	6 h	34 770 ± 900

Determination of caspase-3 activity in lipofectin, mismatch 1132 or SAO 903-, 904-treated MSN neuroblastoma cells. Staurosporine treatment served as positive control for caspase-3 activity in MSN cells. Caspase activity was determined by measuring the cleavage of the caspase-3 fluorescence substrate Ac-DEVD-AMC. Caspase-3 activity was expressed as mean relative fluorescence units/mg protein ± SD. All values were assayed in triplicate.

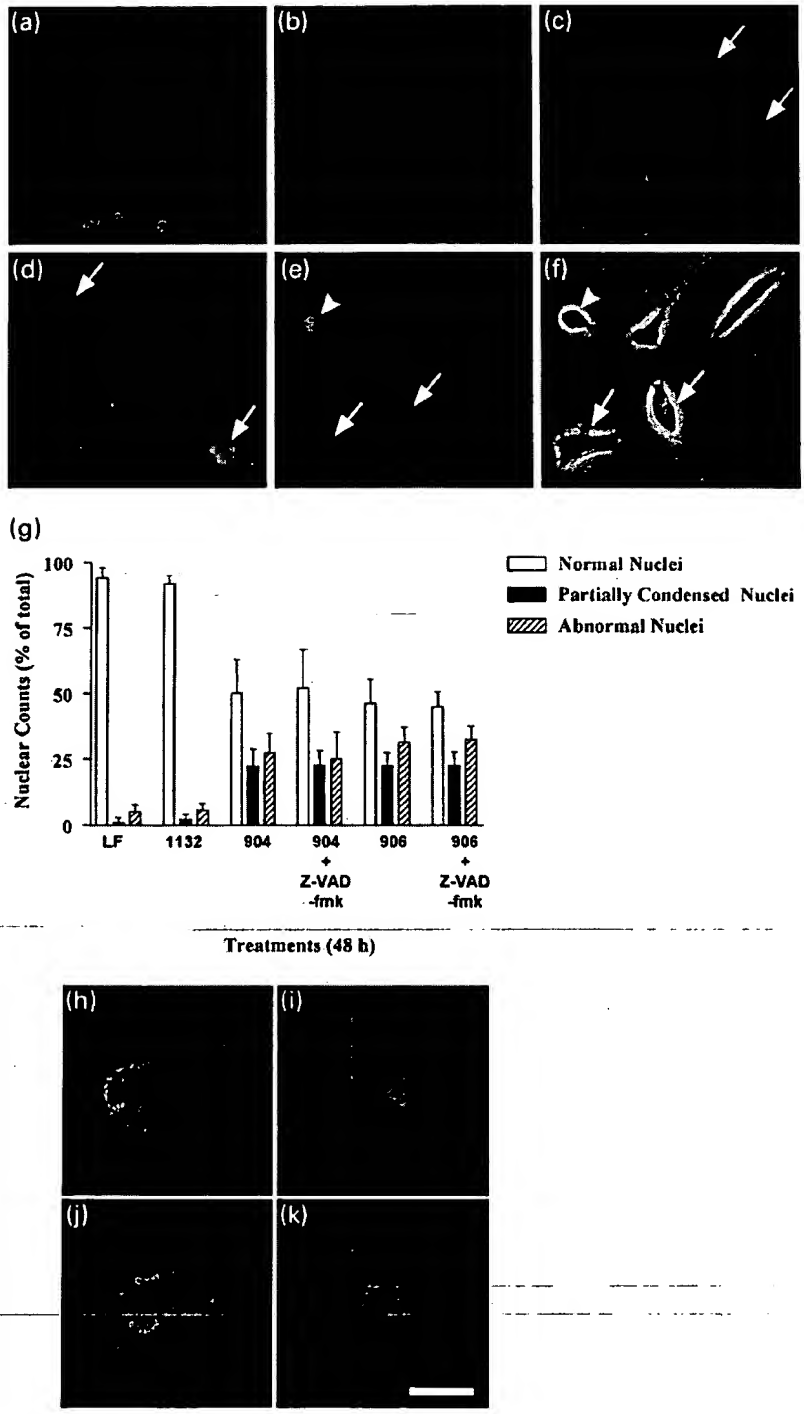

Fig. 4 SAO-treated MSN cells undergo caspase-independent nuclear morphologic changes. MSN cells were treated with lipofectin (a), 600 nM of mismatch 1132 (b), or SAO 904 (c and e), 906 (d) and stained with PI. Arrows in panels (c), (d), (e) and (f) point to abnormal multiple multilobed nuclei. Panel (f) shows the phase of panel (e) demonstrating that the abnormal multilobed nuclei are present within individual cells. The arrowhead in panel (e) shows a partially condensed nuclei. Two independent experiments were performed in duplicate. (g) Co-administration of SAO and zVAD-fmk does not alter the nuclear morphology in SAO-treated MSN cells. MSN cells were treated with 600 nM SAO 904, 906 or mismatch 1132 alone, or in the presence of 20 μM of zVAD-fmk and stained with PI. Approximately 500–600 nuclei were scored on 15 random 40 × objective fields in duplicate as described. The experiment was performed twice and the results are mean ± SEM obtained from the two independent experiments. (h–k) SAO-treated MSN cells show nuclear translocation of AIF. Lipofectin-treated MSN cells (h), MSN cells treated with 600 nM SAO 904 (i), mismatch 1132 (j) or SAO 906 (k) were double-labeled with AIF and DAPI. Note that in the SAO–treated cells the nuclei are pink when the AIF (red) and the DAPI (blue) colocalize. Photomicrographs are from a representative experiment performed in duplicate and similar results were obtained in an additional experiment. Scale bar = 20 μm.

arrows) and abnormally large nuclei (Fig. 4d) consistent with cells blocked in cell division when the nuclear membrane reassociated. Quantitation of the SAO 904 and 906 determined that the percentage of cells with this abnormal nuclear morphology were 27% and 31%, respectively, and this percentage was unaltered in cells co-treated with SAO and zVAD-fmk (Fig. 4g). While no apoptotic bodies or chromatin fragmentation were observed in the SAO-treated cells, 22% of the SAO-treated cells contained nuclei with partially condensed chromatin (Fig. 4e, arrowhead; Fig. 4g) and the percentage did not differ with zVAD-fmk treatment. Thus, approximately 50% of the SAO-treated cells contained

abnormal nuclei and condensed chromatin. The partially condensed chromatin is inconsistent with necrotic cell death and is suggestive of cells undergoing but not completing apoptotic cell death.

Apoptotic cell bodies and further condensation of the cell requires activated caspases and our data indicates that the existing phenotypes are caspase-independent even upon prolonged (≥ 72 h) SAO exposure. In cells undergoing death by a caspase-independent mechanism apoptosis-inducing factor (AIF) is translocated from the mitochondria to the nucleus prior to cytochrome *c* release from the mitochondria and concomitant partial chromatin condensation is observed (Daugas *et al.* 2000). To examine whether down-regulation of survivin induces AIF nuclear translocation, AIF and DAPI double-labeling was performed on SAO-treated MSN cells. As shown in Fig. 4(h and j), both lipofectin-treated and mismatch oligonucleotide 1132 treated cells show robust AIF staining in the cytosol. Only 4–8% of the cells contained nuclear localization of AIF, and DAPI staining showed that 95% of the cells had normal appearing nuclei. By contrast, 45–51% of SAO 904- and 906-treated cells showed AIF nuclear translocation (Figs 4i and k). DAPI staining indicated that 37% of these SAO-treated cells contained partially condensed chromatin, and 25% had abnormal nuclei similar to the PI staining in Fig. 4(g). The lack of highly condensed apoptotic bodies, the nuclear translocation of AIF, and the morphologic appearance of the nuclei by PI and DAPI are consistent with cells undergoing cell death by a caspase-independent mechanism. Thus, the combined PI, DAPI and AIF data is consistent with a disruption in the cell cycle, likely mitotic catastrophe, resulting in cell death.

Increase in XIAP levels following SAO treatment of MSN cells

We considered why caspase-3 was inactive and PARP was not cleaved following SAO treatment of the MSN cells. We speculated that during the SAO treatment another IAP family member might be activated and effectively blocking caspase activation and subsequently PARP cleavage. Therefore, following SAO treatment, XIAP, another member of the IAP family was examined by immunoblotting. As shown in Fig. 5, an eight-fold increase in XIAP was observed in MSN cells 48 h following treatment with SAO 904 while the lipofectin-treated MSN cells had low XIAP levels. This suggests that a dramatic increase of XIAP observed in MSN cells may account for possible inhibition of caspase activation.

Apoptotic cell death in the TC620 oligodendroglioma following SAO treatment

Transfection of TC620 cells with SAO 904 induced a concentration-dependent reduction in survivin protein levels and at 400 nM, a 54% decrease relative to lipofectin-treated cells was observed (Fig. 6a). To determine whether the decrease in survivin was associated with an apoptotic mode of cell death, PARP cleavage was examined by immunoblotting. SAO treatment induced PARP cleavage and generated the 85-kDa fragment characteristic of caspase induction during apoptosis. At concentrations of 100–400 nM SAO 904, a dramatic decrease of the 116-kDa PARP protein and an increase of the 85-kDa cleaved fragment was seen relative to the cleaved fragment seen in the lipofectin-treated cells and untreated cells. PARP cleavage in the lipofectin-treated (Fig. 6b) and untreated cells reflects the basal level of spontaneous apoptosis (Yang *et al.* 2000) in the TC620 cells prior to survivin antisense treatment. These experiments demonstrated that inhibition of survivin expression with SAO treatment is sufficient to induce apoptotic cell death in the TC620 cells.

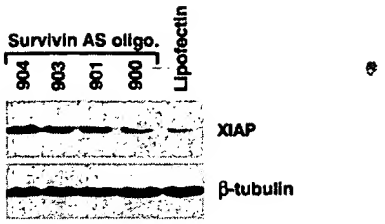

Fig. 5 XIAP was increased in MSN cells following SAO treatment. Cells were treated with lipofectin or 400 nM of SAO 900, 901, 903 and 904 for 48 h. The blot was sequentially incubated with a XIAP monoclonal antibody (1 : 1000; IgG_1) and β-tubulin (1 : 1000). Experiment was performed twice. With SAO treatment, the change of XIAP protein over β-tubulin relative to lipofectin was: 900, 2.3-fold; 901, 3.9-fold; 903, 5.2-fold; 904, 8.0-fold. The result is representative of a single experiment. Similar results were obtained in an additional experiment.

Trypan blue cell viability assays confirmed that SAO 904 induced a concentration-dependent increase in trypan blue-positive cells after 48 h treatment (Fig. 6c). At 100 nM, 200 nM and 400 nM the percentage of dead cells was 28%, 36%, and 62%, respectively. The percentage of trypan blue-positive cells treated with 600 nM mismatched oligonucleotide 1132 (8%) was similar to the lipofectin control (6%). As shown in Fig. 6(d), the percentages of trypan blue positive cells with SAO 904 and 906 at 600 nM concentration was 70% and 67%, respectively, and zVAD-fmk effectively decreased the numbers of trypan blue positive cells induced by SAO treatment to 11% and 15% further supporting a caspase-dependent mechanism of apoptotic cell death in the SAO-treated TC620 cells.

To confirm the results of the PARP data that survivin down-regulation induced apoptosis, a TUNEL assay was performed on lipofectin, mismatch oligonucleotide 1132 and SAO-treated TC620 cells. The percentages of TUNEL positive cells with SAO 904 and 906 at 400 nM concentration was 52% and 54%, respectively. At 600 nM, 63% of

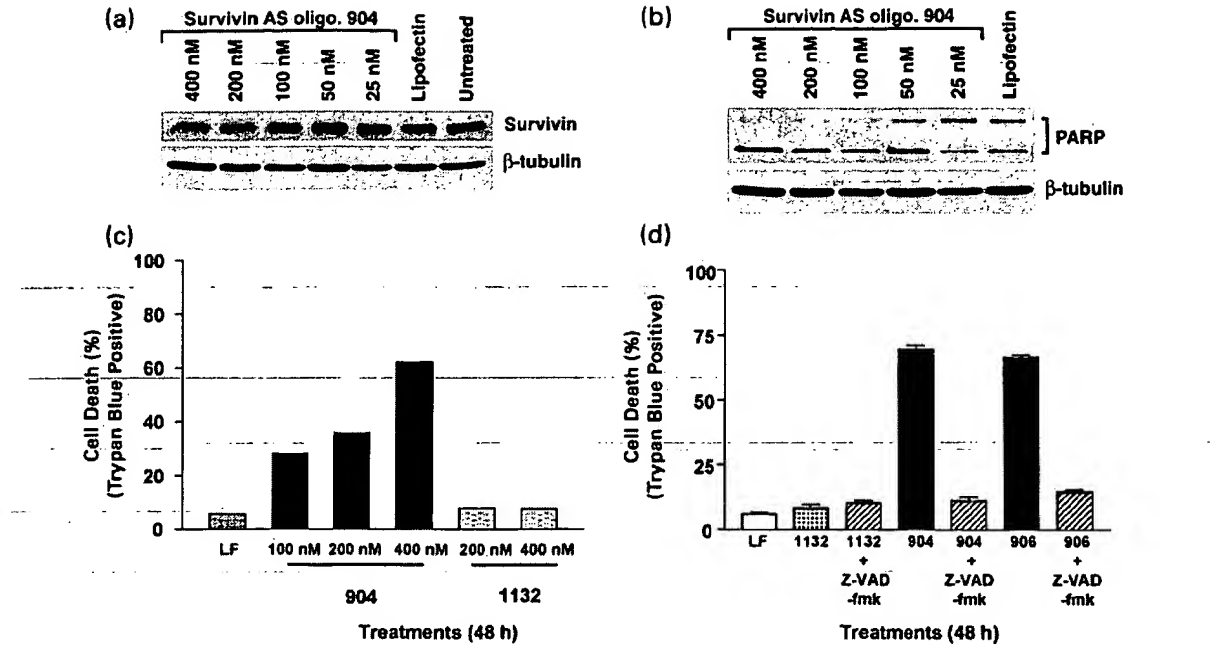

Fig. 6 SAO reduced survivin protein levels and induced apoptosis in TC620 cells. All experiments were performed at least twice. (a) TC620 cells were treated with lipofectin or increasing concentrations of SAO 904 (25–400 nM) for 48 h. The percentage of survivin protein over β-tubulin relative to lipofectin upon treatment with SAO 904 was: 25 nM, 109.1%; 50 nM, 97.4%; 100 nM, 67.6%; 200 nM, 45.2%; 400 nM, 45.7%. (b) PARP is cleaved in TC620 cells following SAO treatment. The blot was incubated with a PARP monoclonal antibody (1 : 500) and visualized by ECL. (c) TC620 cells were treated with lipofectin, SAO 904 at 100, 200 and 400 nM or mismatched oligonucleotide 1132 at 200 nM and 400 nM concentrations, and stained with trypan blue. All time points were calculated in triplicate. (d) TC620 cells were treated with lipofectin, 600 nM SAO 904, 906 or mismatch oligonucleotide 1132 alone, or co-treated with 20 μM of zVAD-fmk as above. Data represent mean ± SEM obtained from two independent experiments performed in duplicate.

SAO 904- and 906-treated TC620 cells were TUNEL positive. Only 4% of the cells were TUNEL positive in the presence of lipofectin or mismatch oligonucleotide 1132.

PI staining of lipofectin or mismatch oligonucleotide 1132 treated TC620 cells showed normal nuclear morphology (Figs 7a and b) with very few apoptotic cells (2%) or cells with abnormal nuclei (1%; Fig. 8a). By contrast, 40–43% of the SAO-treated TC620 cells revealed nuclei with chromatin fragmentation and apoptotic bodies characteristic of an apoptotic mode of cell death (Fig. 7c, arrows; Fig. 8a). In addition, 9% of the SAO-treated cells exhibited multiple multilobed nuclei (Figs 7d and e, arrows; Fig. 8a). Thus,

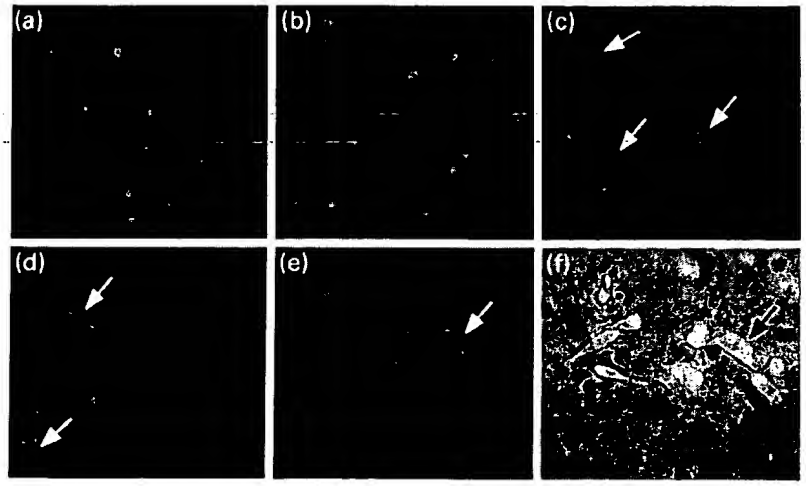

Fig. 7 PI staining demonstrates abnormal nuclear morphology of TC620 cells following SAO treatment. TC620 cells were treated with lipofectin (a), 600 nM of mismatch 1132 (b) or SAO 904 (c and e), 906 (d) and stained with PI. Arrows in panel (c) point to apoptotic nuclei, and in panels (d), (e) and (f) point to abnormal macronuclei that are multi-lobed. Panel (f) shows phase micrograph of panel (e) demonstrating that the abnormal multilobed nuclei are within individual cells. Two independent experiments were performed in duplicate.

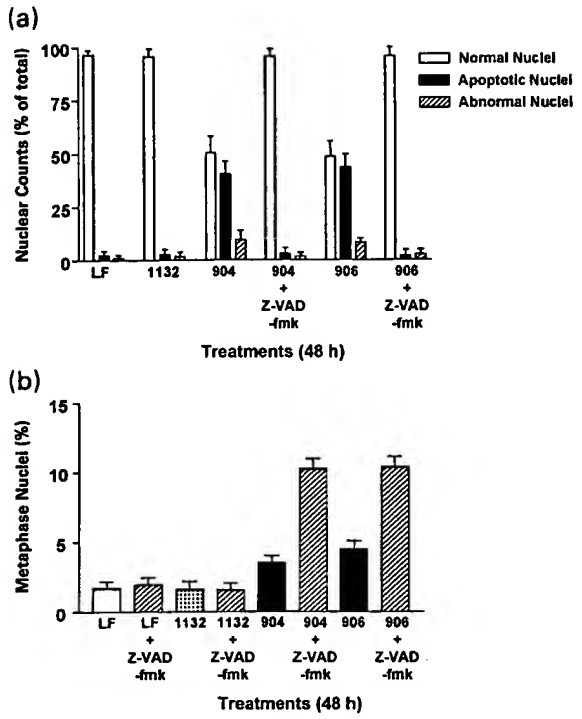

Fig. 8 Analysis of SAO-treated TC620 cells following PI treatment. (a) TC620 cells were treated with 600 nM SAO 904, 906, mismatch 1132, or in the presence of zVAD-fmk. Approximately, 500–600 nuclei were scored as normal, apoptotic or abnormal (macronuclei, multilobed) on 15 random 40 × objective fields in duplicate following PI staining. (b) TC620 cells were treated as described in (a) were stained with PI. Cells in metaphase were identified as those with chromosomes aligned on the metaphase plate; 15 random 40 × objective fields were counted. Results are mean ± SEM obtained from two independent experiments performed in duplicate.

49–52% of the SAO-treated TC620 cells had abnormal nuclei. Co-treatment with SAO and zVAD-fmk dramatically inhibited apoptosis and the abnormal nuclear morphology (Fig. 8a) indicating that down-regulation of survivin results in caspase activation and apoptosis. Taken together, the 85-kDa PARP cleavage product, PI staining of apoptotic bodies, zVAD-fmk inhibition of cell death and TUNEL staining of apoptotic cells definitively established apoptotic cell death in the survivin down-regulated TC620 cells.

Co-administration of SAO and the caspase inhibitor zVAD-fmk decreased the numbers of abnormal nuclei from >40% to 2% (Fig. 8a). Microscopic assessment of the SAO plus zVAD-fmk-treated cells demonstrated an approximate two-fold increase in the number of cells in metaphase compared with cells treated with SAO 904 or 906 alone (Fig. 8b). zVAD-fmk in the presence of lipofectin and mismatch 1132 did not affect the number of cells in metaphase. This suggests that in the absence of survivin, SAO-treated TC620 cells cannot complete the normal mitotic cycle, arrest in metaphase and subsequently undergo apoptosis as a result of mitotic catastrophe. Our results support an interplay between mitotic regulation, tumor survival and cell death.

Discussion

In this study, we have shown that all of the brain tumor cell lines examined in our laboratory expressed survivin. While the neuroblastoma, glioblastoma and the astrocytoma cells showed comparable survivin expression, the presence and abundance of survivin is indicative of a role for survivin as a regulator of neural tumor survival and pathogenesis. Precisely, how survivin regulates tumor progression is not completely understood, however it is clear from both the MSN and TC620 cell lines that survivin plays a major role in progression through mitosis.

Our results show that inhibition of survivin resulted in a dramatic increase in macronuclei and multinucleated cells in the SAO-treated MSN cells relative to the scrambled oligonucleotide-treated cells or the untreated cells consistent with failed cytokinesis. PI staining and flow cytometry could not definitively demonstrate changes in ploidy due to the existing aneuploidy of MSN cells (54–96 chromosomes; Shafit-Zagardo, unpublished observation). Our studies are consistent with other reports that showed that SAO treatment results in cell death (Li *et al.* 1999; Chen *et al.* 2000; Olie *et al.* 2000), however, in the MSN cells SAO treatment did not activate caspase-3 or cleave PARP, and zVAD-fmk did not alter cell death suggesting that MSN cells die by a caspase-independent pathway. Our observation that the percentage of cell death in the SAO-treated MSN cells was unaltered in the presence of zVAD-fmk (Figs 3c and 4g) further supports our finding that caspase-3 was not activated upon SAO treatment. This result led us to speculate that MSN cells suppress caspase activation by the activation of another caspase binding protein. XIAP, c-IAP-1, c-IAP-2 and livin have the ability to interact directly with caspases and inhibit their ability to cleave substrates (Deveraux *et al.* 1997; Roy *et al.* 1997; Kasof and Gomes 2000). XIAP is considered to be the strongest inhibitor of caspase-3 activation (Datta *et al.* 2000). Therefore, we examined XIAP and determined that SAO treatment resulted in a dramatic increase in XIAP. This demonstrates that MSN cells and likely other tumor types can compensate for the loss of survivin function by up-regulating other IAP family members. Since these cells still underwent cell death indicates that survivin's main role in MSN cells is in cell cycle progression, and the possible inhibition of caspases cannot block cell death.

While we did not observe caspase activation or PARP cleavage in MSN cells following SAO treatment, we did observe abnormal nuclei and partial chromatin condensation even in the presence of zVAD-fmk. Partial chromatin

condensation suggests that an early stage of nuclear apoptosis was initiated in the absence of caspase activation (Daugas *et al.* 2000; Susin *et al.* 1999, 2000). Partial chromatin condensation can occur in cells that undergo caspase-independent atypical apoptosis and involves the nuclear translocation of apoptosis-inducing factor (AIF), a mitochondrial intermembrane flavoprotein, resulting in DNA fragmentation (> 50 kb) and partial chromatin condensation similar to the first stage of nuclear apoptosis in intact cells (Susin *et al.* 2000; Joza *et al.* 2001). AIF has been shown to be translocated to the nucleus prior to the release of cytochrome *c* from the mitochondria (Daugas *et al.* 2000). By immunofluorescence, we observed a consistent AIF and cytochrome *c* redistribution pattern in the SAO-treated MSN cells (data not shown). Our data clearly demonstrate that AIF nuclear translocation and ensuing partial chromatin condensation occurs following SAO treatment consistent with caspase-independent cell death.

In contrast to MSN cells, SAO-treated TC620 cells did not up-regulate XIAP and underwent caspase-dependent apoptotic cell death that was blocked when SAO and zVAD-fmk were co-administered. SAO and zVAD-fmk co-treated cells had two-fold more metaphase cells than untreated cells suggesting that the down-regulation of survivin inhibited cell cycle progression and mitotic catastrophe contributed to apoptosis.

Based on our studies, it appears that survivin functions predominantly in cell division. Since cell cycle progression is universal it is not surprising that we observe survivin expression in all neural tumor cells examined. Survivin null mice die in embryogenesis, are polyploid and have disrupted microtubules consistent with a role in cell division (Uren *et al.* 2000). Proteins involved in control of chromosome number or ploidy have been implicated in regulating programmed cell death and survivin may have developed IAP function via its BIR domain to aid in normal cell division and survival. In tumor cells, the death program is often compromised and regulated abnormally by a process of random mutation and selection, becoming progressively more malignant as they accumulate mutations that improve their ability to survive and proliferate. Thus, survivin's role in cell division has been co-opted by the tumor cell to aid in its survival.

Our results indicate that inhibition of survivin expression unequivocally induced cell death in both the neuroblastoma and oligodendroglioma cell lines by a caspase-independent and caspase-dependent mechanism. Following survivin down-regulation, caspase activation appears to be contingent upon the ability of the cell to regulate and alter the levels of other IAP family members, particularly XIAP. This in part also supports the observation that survivin binds quantitatively *in vitro* to an IAP-inhibiting protein Smac/DIABLO (Du *et al.* 2000), raising the possibility that it might suppress caspases indirectly by freeing other IAP family proteins from the constraints of this protein.

Acknowledgements

We thank Ms. M. Heather Knowles for performing the caspase-3 assays. We thank Dr Anthony Sandler, University of Iowa and Dr Dario C. Altieri, Yale University for the pCMV-survivin cDNA construct. This work was supported by the National Institutes of Health Grant R01NS38102 (BS-Z) and by the Albert Einstein College of Medicine Department of Pathology Pilot Project Grant for Postdoctoral Fellows (SLS).

References

Adida C., Berrebi D., Peuchmaur M., Reyes-Mugica M. and Altieri D. C. (1998) Anti-apoptosis gene, survivin, and prognosis of neuroblastoma. *Lancet* **351**, 882–883.

Agrawal S. and Kandimalla E. R. (2000) Antisense therapeutics: is it as simple as complementary base recognition? *Mol. Med. Today* **6**, 72–81.

Albala J. S., Kress Y., Liu W.-K., Weidenheim K., Yen S.-H.C. and Shafit-Zagardo B. (1995) Human microtubule-associated protein-2c localizes to dendrites and axons in fetal spinal motor neurons. *J. Neurochem.* **64**, 2480–2490.

Carlson B. A., Dubay M. M., Sausville E. A., Brizuela L. and Worland P. J. (1996) Flavopiridol induces G1 arrest with inhibition of cyclin-dependent kinase (CDK) 2 and CDK4 in human breast carcinoma cells. *Cancer Res.* **56**, 2973–2978.

Chen J., Wu W., Tahir S. K., Kroeger P. E., Rosenberg S. H., Cowsert L. M., Bennett F., Krajewski S., Krajewska M., Welsh K., Reed J. C. and Ng S. C. (2000) Down-regulation of survivin by antisense oligonucleotides increases apoptosis, inhibits cytokinesis and anchorage-independent growth. *Neoplasia* **2**, 235–241.

Conway E. M., Pollefeyt S., Cornelissen J., DeBaere I., Steiner-Mosonyi M., Ong K., Baens M., Collen D. and Schuh A. C. (2000) Three differentially expressed survivin cDNA variants encode proteins with distinct antiapoptotic functions. *Blood* **95**, 1435–1442.

Datta R., Oki E., Endo K., Biedermann V., Ren J. and Kufe D. (2000) XIAP regulates DNA damage-induced apoptosis downstream of caspase-9 cleavage. *J. Biol. Chem.* **275**, 31733–31738.

Daugas E., Susin S. A., Zamzami N., Ferri K. F., Irinopoulou T., Larochette N., Prevost M. C., Leber B., Andrews D., Penninger J. and Kroemer G. (2000) Mitochondrio-nuclear translocation of AIF in apoptosis and necrosis. *FASEB J.* **14**, 729–739.

Deininger M. H., Weller M., Streffer J. and Meyermann R. (1999) Antiapoptotic Bcl-2 family protein expression increases with progression of oligodendroglioma. *Cancer* **86**, 1832–1839.

Deveraux Q. L., Takahashi R., Salvesen G. S. and Reed J. C. (1997) X-linked IAP is a direct inhibitor of cell-death proteases. *Nature* **388**, 300–304.

Du C., Fang M., Li Y., Li L. and Wang X. (2000) Smac, a mitochondrial protein that promotes cytochrome c-dependent caspase activation by eliminating IAP inhibition. *Cell* **102**, 33–42.

Islam A., Kageyama H., Takada N., Kawamoto T., Takayasu H., Isogai E., Ohira M., Hashizume K., Kobayashi H., Kaneko Y. and Nakagawara A. (2000) High expression of survivin, mapped to 17q25, is significantly associated with poor prognostic factors and promotes cell survival in human neuroblastoma. *Oncogene* **19**, 617–623.

Joza N., Susin S. A., Daugas E., Stanford W. L., Cho S. K., Li C. Y., Sasaki T., Elia A. J., Cheng H. Y., Ravagnan L., Ferri K. F.,

Zamzami N., Wakeham A., Hakem R., Yoshida H., Kong Y. Y., Mak T.W., Zuniga-Pflucker J. C., Kroemer G. and Penninger J. M. (2001) Essential role of the mitochondrial apoptosis-inducing factor in programmed cell death. *Nature* **410**, 549–554.

Kasof G. M. and Gomes B. C. (2000) Livin, a novel inhibitor of apoptosis protein family member. *J. Biol. Chem.* **276**, 3238–3246.

LaCasse E. C., Baird S., Korneluk R. G. and MacKenzie A. E. (1998) The inhibitors of apoptosis (IAPs) and their emerging role in cancer. *Oncogene* **17**, 3247–3259.

Laemmli U. K. (1970) Cleavage of structural proteins during the assembly of the head of the bacteriophage T4. *Nature* **227**, 680–685.

Leaver H. A., Whittle I. R., Wharton S. B. and Ironside J. W. (1998) Apoptosis in human primary brain tumours. *Br. J. Neurosurg.* **12**, 539–546.

Li F., Ambrosini G., Chu E. Y., Plescia J., Tognin S., Marchisio P. C. and Altieri D. C. (1998) Control of apoptosis and mitotic spindle checkpoint by survivin. *Nature* **396**, 580–584.

Li F., Ackermann E. J., Bennett C. F., Rothermel A. L., Plescia J., Tognin S., Villa A., Marchisio P. C. and Altieri D. C. (1999) Pleiotropic cell-division defects and apoptosis induced by interference with survivin function. *Nat. Cell. Biol.* **1**, 461–466.

O'Connor D. S., Grossman D., Plescia J., Li F., Zhang H., Villa A., Tognin S., Marchisio S. and Altieri D. C. (2000) Regulation of apoptosis at cell division by p34cdc2 phosphorylation of survivin. *Proc. Natl Acad. Sci. USA* **97**, 13103–13107.

Olie R. A., Simoes-Wust A. P., Baumann B., Leech S. H., Fabbro D., Stahel R. A. and Zangemeister-Wittke U. (2000) A novel antisense oligonucleotide targeting survivin expression induces apoptosis and sensitizes lung cancer cells to chemotherapy. *Cancer Res.* **60**, 2805–2809.

Reynolds C. P., Biedler J. L., Spengler B. A., Reynolds D. A., Ross R. A., Frenkel E. P. and Smith R. G. (1986) Characterization of human neuroblastoma cell lines established before and after therapy. *J. Natl Cancer Inst.* **76**, 375–387.

Roy N., Deveraux Q. L., Takahashi R., Salvesen G. S. and Reed J. C. (1997) The c-IAP-1 and c-IAP-2 proteins are direct inhibitors of specific caspases. *EMBO J.* **16**, 6914–6925.

Shafit-Zagardo B., Peterson C. and Goldman J. E. (1988) Rapid increases in glial fibrillary acidic protein mRNA and protein levels in the copper-deficient, brindled mouse. *J. Neurochem.* **51**, 1258–1266.

Skoufias D. A., Mollinari C., Lacroix F. B. and Margolis R. L. (2000) Human survivin is a kinetochore-associated passenger protein. *J. Cell. Biol.* **151**, 1575–1581.

Susin S. A., Lorenzo H. K., Zamzami N., Marzo I., Snow B. E., Brothers G. M., Mangion J., Jacotot E., Costantini P., Loeffler M., Larochette N., Goodlett D. R., Aebersold R., Siderovski D. P., Penninger J. M. and Kroemer G. (1999) Molecular characterization of mitochondrial apoptosis-inducing factor. *Nature* **397**, 441–446.

Susin S. A., Daugas E., Ravagnan E., Samejima K., Zamzami N., Loeffler M., Costantini P., Ferri K. F., Irinopoulou T., Prevost M.C., Brothers G., Mak T. W., Penninger J., Earnshaw W. C. and Kroemer G. (2000) Two distinct pathways leading to nuclear apoptosis. *J. Exp. Med.* **192**, 571–579.

Suzuki A., Hayashida M., Ito T., Kawano H., Nakano T., Miura M., Akahane K. and Shiraki K. (2000) Survivin initiates cell cycle entry by the competitive interaction with Cdk4/p16 (INK4a) and Cdk2/cyclin E complex activation. *Oncogene* **19**, 3225–3234.

Towbin H., Staehelin T. and Gordon J. (1979) Electrophoretic transfer of proteins from polyacrylamide gels to nitrocellulose sheets: procedure and some applications. *Proc. Natl Acad. Sci. USA* **76**, 4350–4354.

Uren A. G., Wong L., Pakusch M., Fowler K. J., Burrows F. J., Vaux D. L. and Choo K. H. A. (2000) Survivin and the inner centromere protein INCENP show similar cell-cycle localization and gene knockout phenotype. *Curr. Biol.* **10**, 1319–1328.

Yang Y., Fang S., Jensen J. P., Weismann A. M. and Ashwell J. D. (2000) Ubiquitin protein ligase activity of IAPs and their degradation in proteasomes in response to apoptotic stimuli. *Science* **288**, 874–877.